Published OnlineFirst May 25, 2010; DOI: 10.1158/0008-5472.CAN-10-0120

Priority Report

Cancer Research

Histone Methyltransferase Gene *SETD2* Is a Novel Tumor Suppressor Gene in Clear Cell Renal Cell Carcinoma

Gerben Duns[1], Eva van den Berg[1], Inge van Duivenbode[1], Jan Osinga[1], Harry Hollema[2], Robert M.W. Hofstra[1], and Klaas Kok[1]

Abstract

Sporadic clear cell renal cell carcinoma (cRCC) is genetically characterized by the recurrent loss of the short arm of chromosome 3, with a hotspot for copy number loss in the 3p21 region. We applied a method called "gene identification by nonsense-mediated mRNA decay inhibition" to a panel of 10 cRCC cell lines with 3p21 copy number loss to identify biallelic inactivated genes located at 3p21. This revealed inactivation of the histone methyltransferase gene *SETD2*, located on 3p21.31, as a common event in cRCC cells. *SETD2* is nonredundantly responsible for trimethylation of the histone mark H3K36. Consistent with this function, we observed loss or a decrease of H3K36me3 in 7 out of the 10 cRCC cell lines. Identification of missense mutations in 2 out of 10 primary cRCC tumor samples added support to the involvement of loss of *SETD2* function in the development of cRCC tumors. *Cancer Res; 70(11); 4287–91. ©2010 AACR.*

Introduction

Clear cell renal cell carcinoma (cRCC) is the most prevalent subtype of renal cell carcinoma and accounts for 3% of all human malignancies (1). Originating from the epithelium of the proximal tubulus, it is genetically characterized by recurrent loss of 3p regions. These losses are thought to represent one of the two hits required to functionally inactivate tumor suppressor genes (TSG) located in these regions (2). The *Von Hippel-Lindau* gene, located at 3p25, has been identified as a TSG involved in the pathology of cRCC, and is inactivated in the majority (57–80%) of cRCCs (3, 4). Although the frequent copy number loss of 3p21 (5) also suggests the presence of one or more additional TSGs in this segment of 3p, decades of research have not led to the identification of a TSG located in this genomic segment. In an attempt to identify a putative 3p21 TSG, we applied a modified version of the "gene identification by nonsense-mediated mRNA decay inhibition" (GINI) method (6) to a panel of 10 cRCC cell lines showing copy number loss of 3p21. The GINI method allows for genome-wide identification of transcripts harboring premature termination codons (PTC). Inhibition of the nonsense-mediated mRNA decay pathway *in vitro* results in the accumulation of PTC transcripts, which can be detected using gene expression microarrays. Several groups have successfully applied modified versions of the GINI method in their search for TSGs (7–9). Using GINI, we identified the histone methyltransferase gene *SETD2/HYPB*, located on 3p21.31, as a new TSG involved in the development of cRCC.

Materials and Methods

Cell lines

cRCC cell lines RCC-AB, RCC-ER, RCC-FG2, RCC-HS, RCC-JF, RCC-JW, RCC-MF, and RCC-WK were obtained from Cell Line Services, Eppenheim, Germany. The cells, which tested negatively for *Mycoplasma*, bacteria, and fungi, had been passed 10 to 13 times upon arrival (as stated by Cell Line Services). Experiments were performed on cells that had undergone six to eight additional passages. cRCC cell lines RCC-1, RCC-4, and RCC-5 were established by Dr. C.D. Gerharz (Institute of Pathology, University Hospital, Düsseldorf, Germany) and karyotyped. To ensure their authenticity, they were recently re-karyotyped. All cRCC cell lines were maintained in RPMI 1640 (Sigma). Embryonal kidney cell line HEK293T was obtained from American Type Culture Collection (CRL-1573) and maintained in DMEM (Sigma). MN160 and PTEC are primary cultures derived from proximal tubular epithelial cells. DNA was purified using a phenol/chloroform extraction method.

Primary tumor samples

Primary cRCC tumor samples (for details, see Supplementary Table S1) were snap-frozen in liquid nitrogen, sections were cut and the histology was reviewed by a pathologist (H. Hollema). Tissue biopsies containing at least 70% tumor cells were selected for analysis. DNA was isolated using the QIAamp DNA Micro Kit (Qiagen). DNA samples from

Authors' Affiliations: Departments of [1]Genetics and [2]Pathology, University Medical Centre Groningen, University of Groningen, Groningen, the Netherlands

Note: Supplementary data for this article are available at Cancer Research Online (http://cancerres.aacrjournals.org/).

Corresponding Author: Klaas Kok, Department of Genetics, University Medical Centre Groningen, P.O. Box 30001, 9700 RB Groningen, the Netherlands. Phone: 31-50361-7100; Fax: 31-50361-7230; E-mail: k.kok@medgen.umcg.nl.

doi: 10.1158/0008-5472.CAN-10-0120

Published OnlineFirst May 25, 2010; DOI: 10.1158/0008-5472.CAN-10-0120

formalin-fixed matching normal kidney samples were obtained using a paraffin material DNA isolation protocol.

ArrayCGH

ArrayCGH was carried out using Agilent Human Genome CGH Microarray 244a slides (p/n G4411B) following the protocols of the manufacturer. Slides were scanned using the G25052C DNA microarray scanner (Agilent Technologies). Array images were analyzed using Agilent feature extraction software (v10.5.1.1) and DNA analytics (Agilent).

GINI

Cells were grown to 70% confluence and treated with emetine dihydrochloride hydrate (100 μg/mL medium) or caffeine (10 mmol/L in medium), or not treated. Following 8 hours of incubation at 37°C, cells were harvested. Experiments were performed in duplicate. RNA was isolated using the RNeasy Mini Kit (Qiagen). Transcript abundance in treated and untreated cells was measured using Human HT-12_V3_Beadchips (48K; Illumina). The Lumi package implemented in R (10, 11) was used for variance stabilizing transformation followed by robust spline normalization of the microarray data (GEO accession no. GSE20491). GeneSpring GX 10.0 (Agilent) was used to calculate treatment-induced fold changes. Putative PTC-containing transcripts were selected according to the following criteria:

1. Transcripts should show emetine- as well as caffeine-induced accumulation in one or more cell lines. Transcripts were considered to be accumulated when present in the list of 1,000 transcripts with the highest treatment-induced fold changes.
2. Transcripts showing accumulation in the majority of cell lines were considered to be so-called stress-response genes and were discarded from further analyses.
3. In untreated cells, PTC transcripts should show a significantly lower abundance than their non-PTC harboring counterparts.
4. Emetine- and caffeine-induced accumulation pushes the abundance towards a level similar to the abundance in PTEC and MN160.

Mutation analysis

Thirty-seven PCR primer sets were designed to amplify and sequence all coding sequences and exon-intron boundaries of *SETD2* annotated in the human genome (National Center for Biotechnology Information). Amplified PCR products were purified using EXOSAP IT (GE Healthcare) and sequenced using BigDye Terminator chemistry (Applied Biosystems). Reaction products were run on the ABI3130XL Genetic Analyzer (Applied Biosystems). Sequences were evaluated using Mutation Surveyor (SoftGenetics LCC). Cancer samples showing putative mutations were re-sequenced to eliminate any potential sequencing artifacts. Primer sequences are listed in Supplementary Table S2. To check for aberrant transcripts, cDNA fragments, obtained by reverse transcription of RNA from the cell lines, were amplified using stepdown PCR (60°C–55°C) and visualized on a 2% agarose gel. Primer sequences are listed in Supplementary Table S2.

Western blot analysis

Cells were lysed in Triton extraction buffer [0.5% Triton X-100 (v/v), 2 mmol/L phenylmethylsulfonyl fluoride, and 0.02% NaN_3 (m/v)]. Histones were isolated by acid extraction O/N in 0.2 N HCl, separated using SDS-PAGE (15%) and transferred to a nitrocellulose membrane. The following primary and secondary antibodies were used for Western analysis: rabbit anti-histone 3 (ab1791, 1:4,000; Abcam), rabbit anti-trimethyl histone H3 (Lys36; ab9050, 1:750; Abcam), rabbit anti–dimethyl-histone H3 (Lys 36; 07-369, 1:2,000; Millipore) and horseradish peroxidase–>conjugated secondary antibody (goat anti-rabbit; Bio-Rad). Positive staining was visualized using ECL solution mixture from Roche. Attached antibodies were stripped from the membrane using Re-Blot Plus Strong Solution (Chemicon/Millipore) to allow reuse of themembrane.

Results and Discussion

ArrayCGH analysis

In our search for candidate TSGs located at 3p21, we decided to include only cRCC-derived cell lines and primary tumor samples that showed copy number loss for 3p21. This selection was based on our arrayCGH data. Seven out of 11 cRCC cell lines and 6 out of 11 cRCC primary tumor samples lost the entire short arm of chromosome 3 (3p). Three cell lines and three primary tumor samples had copy number loss of a part of 3p, with a segment of overlap from 21.4 to 69.6 Mb from pter, including 3p21 but not the *VHL* gene, located at 3p26-p25 (Supplementary Fig. S1). One cell line (RCC-WK) did not show copy number loss of 3p21 and was not considered in the subsequent GINI analysis.

GINI analysis

To identify transcripts harboring PTCs, we performed GINI on 10 cRCC cell lines with copy number loss of 3p21. Gene expression microarrays were used to identify transcripts that were accumulated as a result of nonsense-mediated mRNA decay inhibition (Supplementary Table S3). Transcripts were selected for further analysis based on criteria outlined in Materials and Methods. In this study, we restricted the search for biallelic inactivated transcripts to the 3p21 region. One gene fitting all our criteria was the histone methyltransferase gene *SETD2*, located at 3p21.31. Based on the observed "transcript level profiles", we expected *SETD2* to harbor PTCs in RCC-AB and RCC-ER (Fig. 1).

SETD2 mutation analysis

The presence of PTC-introducing mutations in these two cell lines was confirmed by sequence analysis of all exons and exon-intron boundaries of *SETD2*. A 1-bp deletion resulting in a PTC 42 nucleotides downstream was detected in RCC-AB. In RCC-ER, a nonsense mutation was identified (Fig. 2; Supplementary Fig. S2; Supplementary Table S4). The other cell lines were sequenced for mutations other than those causing PTCs. We identified an in-frame 9-bp deletion in exon

Published OnlineFirst May 25, 2010; DOI: 10.1158/0008-5472.CAN-10-0120

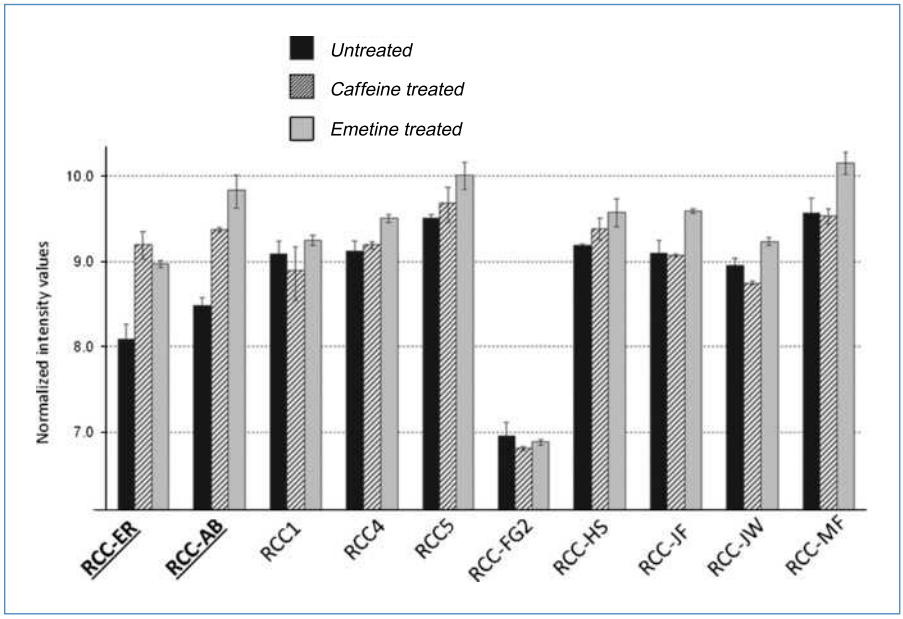

Figure 1. Effect of nonsense-mediated mRNA decay inhibition on *SETD2* transcript levels in cRCC cell lines. For each cell line, *SETD2* transcript levels are shown in untreated (black columns), caffeine-treated (striped columns), and emetine-treated (gray columns) cells, respectively. Normalized intensity values are shown on a log 2 scale. Levels below a value of 7 are close to the detection limit. The *SETD2* probe binds to the 3′ part of the transcript. The *SETD2* transcript in RCC-FG2 lacks this part (Supplementary Fig. S2*i*), explaining the low transcript levels. *SETD2* transcript abundance is low in untreated RCC-AB and RCC-ER cells compared with the other cell lines and shows caffeine- and emetine-induced accumulation in RCC-AB and RCC-ER. Based on these transcript level profiles, we expected RCC-AB and RCC-ER to harbor PTCs in the *SETD2* gene (see also Supplementary Table S3).

11 in RCC-MF, a missense mutation in exon 3 in RCC-JW not corresponding to a known single-nucleotide polymorphism (not present in dbSNP), and a silent mutation in exon 3 in RCC-JF. In addition, the *SETD2* transcript of RCC-FG2 seemed to lack the terminal three exons (Supplementary Fig. S2). To further assess the clinical relevance of these findings, we sequenced *SETD2* in 10 cRCC primary tumors with 3p21 copy number loss (Supplementary Fig. S2), and in two of them, we identified missense mutations that did not correspond to known single-nucleotide polymorphisms (dbSNP).

The mutations identified in RCC-AB, RCC-ER, and RCC-MF as well as the aberrant splicing observed in RCC-FG2 will all have a severe effect on the function of the protein. The three missense mutations identified affect amino acids that are conserved across SETD2 orthologues in several species (Supplementary Fig. S3). The missense mutation in T-3 affects the SET domain, which is responsible for the methyltransferase activity of the protein. The missense mutation in T-4 affects the low charge region, which is thought to have transcriptional activation activity, whereas the missense mutation in RCC-JW affects an amino acid which is not located in a known functional domain (Fig. 2). The missense mutation in T-3 was shown to be somatic (Supplementary Fig. S2). The matching normal renal sample of T-4 was heterozygous for the missense mutation, indicating that *SETD2* mutations might contribute to genetic susceptibility for cRCC. The missense mutations in T-4 and RCC-JW were not seen in 100 healthy control samples. AGVGD, SIFT, and Polyphen gave ambiguous results in their predictions of the pathogenicity of the mutations (Supplementary Table S5). However, the ratio between observed nonsynonymous and synonymous mutations (6:1) was higher than the 2:1 predicted for nonselected passenger mutations (12), indicating that the observed mutations are functional rather than coincidental. The observed mutation frequency in the cRCC primary tumor samples might be an underestimation of the actual frequency, as the samples were not checked for aberrant splicing caused by intronic mutations. Our findings were confirmed by a massive sequencing project on cRCC performed recently that found somatic truncating mutations in *SETD2* in 12 out of 407 (3%) cRCC clinical

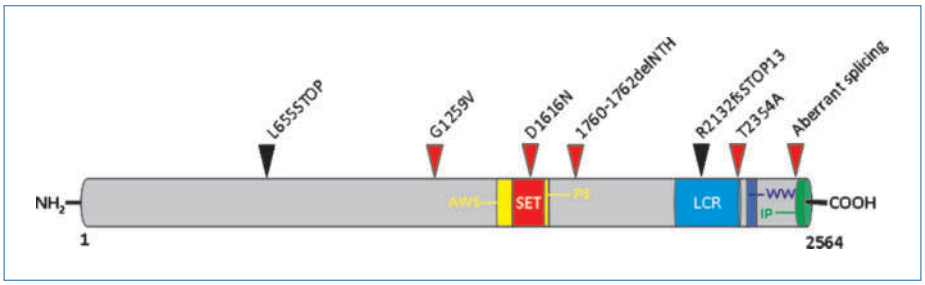

Figure 2. SETD2 mutations in cRCC samples. Schematic representation of SETD2 with arrows showing the locations of the mutations and the corresponding amino acid changes. AWS, AWS domain; SET, SET domain; PS, post-SET domain; LCR, low-charge region; WW, WW domain; IP, interaction with *RNAPOL2A*; Del, deletion. National Center for Biotechnology Information Reference Sequence: NP_054878.5.

Published OnlineFirst May 25, 2010; DOI: 10.1158/0008-5472.CAN-10-0120

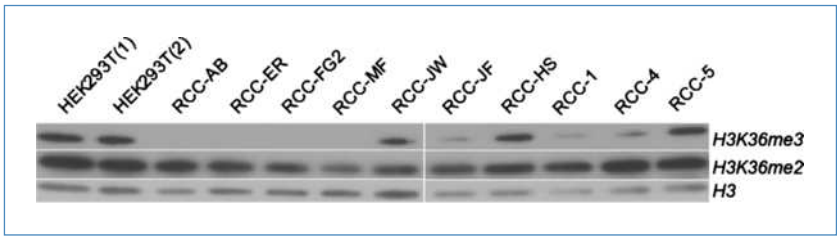

Figure 3. Global histone methylation levels in cRCC cell lines. Global H3K36me3 and H3K36me2 levels in cRCC-derived cell lines as detected by Western blot analysis. HEK293T samples were included as positive controls. Histone 3 (H3) levels were used as a loading control.

specimens (13). Sequencing of a panel of nine small cell lung carcinoma–derived cell lines, a type of carcinoma also characterized by loss of 3p21 (14), did not reveal any hemizygous mutations (data not shown). This implies that the inactivating mutations of *SETD2* could be specific for cRCC, as is also suggested by Dalgliesh and colleagues (13).

Trimethylation of H3K36 in cRCC

SETD2 was discovered in 1998 and initially characterized as Huntingtin-interacting protein (HYPB; refs. 15, 16). In 2005, HYPB was shown to function as a histone methyltransferase via a conserved SET domain and was renamed SETD2 ([Su(var)3–9, enhancer of zeste [E(z)] and trithorax (trx)] domain–containing protein 2). A number of recent articles correlate loss- or gain-of-function of histone-modifying enzymes, including histone lysine methyltransferases, with the pathology of several types of cancer. Aberrant activity of histone-modifying enzymes could result in altered chromatin configuration and disruption of normal transcriptional programs, pushing the cell towards cancerous development (17). Recently, a trend for lower *SETD2* transcript levels in breast cancer tissue was shown, linking the reduction of *SETD2* mRNA levels with tumor development (18). SETD2 is nonredundantly responsible for all trimethylation of lysine 36 of histone H3 (19, 20). This mark may be involved in transcriptional elongation and splicing (21). To assess the effect of the mutations identified in *SETD2* on the global level of trimethylated H3K36, we performed Western blot analysis on our panel of cRCC cell lines. There was a strong decrease of global H3K36me3 levels in 7 out of 10 tested cRCC cell lines, whereas H3K36me2 levels were consistent across the panel of cell lines (Fig. 3). In RCC-ER and RCC-AB, which harbor hemizygous mutations introducing PTCs in SETD2, H3K36me3 was lost. The observed faint residual staining was probably an effect of nonspecific binding of the antibody. RCC-MF and RCC-FG2 have trimethylated H3K36 levels similar to those observed in RCC-AB and RCC-ER, indicating that the mutations in these cell lines totally disrupt the H3K36me3 methyltransferase activity of the SETD2 protein as well. The missense mutation identified in RCC-JW seems to have no effect on the H3K36me3 activity of the SETD2 protein, as the level of global trimethylated H3K36 was not decreased in this cell line. Given the decrease of global trimethylated H3K36 levels in a large subset of our cRCC cell line panel, global H3K36me3 might play a tumor-suppressive role in proximal epithelial tubular cells. The observed decrease of global trimethylated H3K36 in cRCC cell lines in which no mutations in *SETD2* were identified implies that, besides the loss of methyltransferase activity of SETD2, other mechanisms might also result in the loss of H3K36me3. Altogether, our results provide a strong basis for the involvement of loss of SETD2 function in the development of cRCC.

Disclosure of Potential Conflicts of Interest

No potential conflicts of interest were disclosed.

Grant Support

Dutch Cancer Society grant 2007-3892.

The costs of publication of this article were defrayed in part by the payment of page charges. This article must therefore be hereby marked *advertisement* in accordance with 18 U.S.C. Section 1734 solely to indicate this fact.

Received 01/15/2010; revised 03/08/2010; accepted 03/25/2010; published OnlineFirst 05/25/2010.

References

1. Jemal A, Siegel R, Ward E, Hao Y, Xu J, Thun MJ. Cancer statistics, 2009. CA Cancer J Clin 2009;59:225–49.
2. Knudson AG, Jr. Mutation and cancer: statistical study of retinoblastoma. Proc Natl Acad Sci U S A 1971;68:820–3.
3. Gnarra JR, Tory K, Weng Y, et al. Mutations of the *VHL* tumor suppressor gene in renal carcinoma. Nat Genet 1994;7:85–90.
4. Nickerson ML, Jaeger E, Shi Y, et al. Improved identification of von Hippel-Lindau gene alterations in clear cell renal tumors. Clin Cancer Res 2008;14:4726–34.
5. Van den Berg A, Dijkhuizen T, Draaijers TG, et al. Analysis of multiple renal cell adenomas and carcinomas suggests allelic loss at 3p21 to be a prerequisite for malignant development. Genes Chromosomes Cancer 1997;19:59–76.
6. Noensie EN, Dietz HC. A strategy for disease gene identification through nonsense mediated mRNA decay inhibition. Nat Biotechnol 2001;19:434–9.
7. Ionov Y, Nowak N, Perucho M, Markowitz S, Cowell JK. Manipulation of nonsense decay identifies gene mutations in colon cancer cells with microsatellite instability. Oncogene 2004;23:639–45.
8. Huusko P, Poncinano-Jackson D, Wolf M, et al. Nonsense-mediated decay microarray analysis identifies mutation of EPHB2 in human prostate cancer. Nat Genet 2004;36:979–83.
9. Muggerud AA, Edgren H, Wolf M, et al. Data integration from two microarray platforms identifies bi-allelic inactivation of RIC8A in a breast cancer cell line. BMC Med Genet 2009;2:26–34.

Published OnlineFirst May 25, 2010; DOI: 10.1158/0008-5472.CAN-10-0120

10. Du P, Jibbe WA, Lin SM. Lumi: a pipeline for processing Illumina microarray. Bioinformatics 2008;59:1547–8.
11. Lin SM, Du P, Huber W, Kibbe WA. Model-based variance-stabilizing transformation for Illumina microarray data. Nucleic Acids Res 2008; 36:e11.
12. Bardelli A, Parsons D, Silliman N, et al. Mutational analysis of the tyrosine kinome in colorectal cancers. Science 2003;300:949.
13. Dalgliesh GL, Furge K, Greenman C, et al. Systematic sequencing of renal carcinoma reveals inactivation of histone modifying enzymes. Nature 2010;463:360–3.
14. Kok K, Osinga J, Carritt B, et al. Deletion of a DNA sequence at the chromosomal region 3p21 in all major types of lung cancer. Nature 1987;330:578–81.
15. Mao M, Fu G, Wu J-S, et al. Identification of genes expressed in human $CD34^+$ hematopoietic stem/progenitor cells by expressed sequence tags and efficient full-length cDNA cloning. Proc Natl Acad Sci U S A 1998;95:8175–80.
16. Rega S, Stiewe T, Chang D-I, et al. Identification of the full-length huntingtin-interacting protein p231HBP/HYPB as a DNA binding factor. Moll Cell Neurosci 2001;18:68–79.
17. Miremadi A, Oestergaard MZ, Pharoah PDP, Caldas C. Cancer genetics of epigenetic genes. Hum Mol Genet 2007;16:Spec No. 1:R28–49.
18. El Sarakbi W, Sasi W, Jiang WG, Roberts T, Newbold RF, Mokbel K. The mRNA expression of SETD2 in human breast cancer: correlation with clinico-pathological parameters. BMC Cancer 2009;9:290–6.
19. Edmunds JW, Mahadevan LC, Clayton AL. Dynamic histone H3 methylation during gene induction: HYPB/SETD mediates all H3K36 trimethylation. EMBO J 2008;27:406–20.
20. Yoh SM, Lucas JS, Jones KA. The Iws1:Spt6:CTD complex controls cotranscriptional mRNA biosynthesis and HYP/Setd2-mediated histone H3K36 methylation. Gene Dev 2008;22:3422–34.
21. Kolasinska-Zwierz P, Down T, Latorre I, Liu T, Liu XS, Ahringer J. Differential chromatin marking of introns and expressed exons by H3K36me3. Nat Genet 2009;41:376–81.

Cancer Research
The Journal of Cancer Research (1916–1930) | The American Journal of Cancer (1931–1940)

AACR American Association for Cancer Research

Histone Methyltransferase Gene *SETD2* Is a Novel Tumor Suppressor Gene in Clear Cell Renal Cell Carcinoma

Gerben Duns, Eva van den Berg, Inge van Duivenbode, et al.

Cancer Res 2010;70:4287-4291. Published OnlineFirst May 25, 2010.